UCLA
UCLA Previously Published Works

Title
Correlation measurements between flow harmonics in Au+Au collisions at RHIC

Permalink
https://escholarship.org/uc/item/1mj099p5

Authors
Adam, J
Adamczyk, L
Adams, JR
et al.

Publication Date
2018-08-01

DOI
10.1016/j.physletb.2018.05.076

Peer reviewed

Correlation measurements between flow harmonics in Au+Au collisions at RHIC

STAR Collaboration

J. Adam [i], L. Adamczyk [a], J.R. Adams [ad], J.K. Adkins [t], G. Agakishiev [r], M.M. Aggarwal [af], Z. Ahammed [bc], N.N. Ajitanand [aq], I. Alekseev [p,aa], D.M. Anderson [as], R. Aoyama [aw], A. Aparin [r], D. Arkhipkin [c], E.C. Aschenauer [c], M.U. Ashraf [av], F. Atetalla [s], A. Attri [af], G.S. Averichev [r], X. Bai [g], V. Bairathi [ab], K. Barish [ay], A.J. Bassill [ay], A. Behera [aq], R. Bellwied [au], A. Bhasin [q], A.K. Bhati [af], P. Bhattarai [at], J. Bielcik [j], J. Bielcikova [k], L.C. Bland [c], I.G. Bordyuzhin [p], J. Bouchet [s], J.D. Brandenburg [ak], A.V. Brandin [aa], D. Brown [x], J. Bryslawskyj [ay], I. Bunzarov [r], J. Butterworth [ak], H. Caines [bf], M. Calderón de la Barca Sánchez [e], J.M. Campbell [ad], D. Cebra [e], I. Chakaberia [c,s,ao], P. Chaloupka [j], F.-H. Chang [ac], Z. Chang [c], N. Chankova-Bunzarova [r], A. Chatterjee [bc], S. Chattopadhyay [bc], J.H. Chen [ap], X. Chen [v], X. Chen [an], J. Cheng [av], M. Cherney [i], W. Christie [c], G. Contin [w], H.J. Crawford [d], S. Das [g], T.G. Dedovich [r], I.M. Deppner [az], A.A. Derevschikov [ah], L. Didenko [c], C. Dilks [ag], X. Dong [w], J.L. Drachenberg [u], J.C. Dunlop [c], L.G. Efimov [r], N. Elsey [be], J. Engelage [d], G. Eppley [ak], R. Esha [f], S. Esumi [aw], O. Evdokimov [h], J. Ewigleben [x], O. Eyser [c], R. Fatemi [t], S. Fazio [c], P. Federic [k], P. Federicova [j], J. Fedorisin [r], Z. Feng [g], P. Filip [r], E. Finch [ax], Y. Fisyak [c], C.E. Flores [e], L. Fulek [a], C.A. Gagliardi [as], F. Geurts [ak], A. Gibson [bb], D. Grosnick [bb], D.S. Gunarathne [ar], Y. Guo [s], A. Gupta [q], W. Guryn [c], A.I. Hamad [s], A. Hamed [as], A. Harlenderova [j], J.W. Harris [bf], L. He [ai], S. Heppelmann [ag], S. Heppelmann [e], N. Herrmann [az], A. Hirsch [ai], L. Holub [j], S. Horvat [bf], X. Huang [av], B. Huang [h], S.L. Huang [aq], T. Huang [ac], H.Z. Huang [f], T.J. Humanic [ad], P. Huo [aq], G. Igo [f], W.W. Jacobs [o], A. Jentsch [at], J. Jia [c,aq], K. Jiang [an], S. Jowzaee [be], E.G. Judd [d], S. Kabana [s], D. Kalinkin [o], K. Kang [av], D. Kapukchyan [ay], K. Kauder [be], H.W. Ke [c], D. Keane [s], A. Kechechyan [r], D.P. Kikoła [bd], C. Kim [ay], T.A. Kinghorn [e], I. Kisel [l], A. Kisiel [bd], L. Kochenda [aa], L.K. Kosarzewski [bd], A.F. Kraishan [ar], L. Kramarik [j], L. Krauth [ay], P. Kravtsov [aa], K. Krueger [b], N. Kulathunga [au], S. Kumar [af], L. Kumar [af], J. Kvapil [j], J.H. Kwasizur [o], R. Lacey [aq], J.M. Landgraf [c], K.D. Landry [f], J. Lauret [c], A. Lebedev [c], R. Lednicky [r], J.H. Lee [c], Y. Li [av], W. Li [ap], X. Li [an], C. Li [an], J. Lidrych [j], T. Lin [as], M.A. Lisa [ad], Y. Liu [as], H. Liu [o], F. Liu [g], P. Liu [aq], T. Ljubicic [c], W.J. Llope [be], M. Lomnitz [w], R.S. Longacre [c], S. Luo [h], X. Luo [g], R. Ma [c], Y.G. Ma [ap], G.L. Ma [ap], L. Ma [m], N. Magdy [aq], R. Majka [bf], D. Mallick [ab], S. Margetis [s], C. Markert [at], H.S. Matis [w], O. Matonoha [j], D. Mayes [ay], J.A. Mazer [al], K. Meehan [e], J.C. Mei [ao], N.G. Minaev [ah], S. Mioduszewski [as], D. Mishra [ab], S. Mizuno [w], B. Mohanty [ab], M.M. Mondal [n], I. Mooney [be], D.A. Morozov [ah], M.K. Mustafa [w], Md. Nasim [f], T.K. Nayak [bc], J.D. Negrete [ay], J.M. Nelson [d], D.B. Nemes [bf], M. Nie [ap], G. Nigmatkulov [aa], T. Niida [be], L.V. Nogach [ah], T. Nonaka [aw], S.B. Nurushev [ah], G. Odyniec [w], A. Ogawa [c], K. Oh [aj], V.A. Okorokov [aa], D. Olvitt Jr. [ar], B.S. Page [c], R. Pak [c], Y. Panebratsev [r], B. Pawlik [ae], H. Pei [g],

C. Perkins [d], J. Pluta [bd], K. Poniatowska [bd], J. Porter [w], M. Posik [ar], N.K. Pruthi [af],
M. Przybycien [a], J. Putschke [be], A. Quintero [ar], S.K. Radhakrishnan [w], S. Ramachandran [t],
R.L. Ray [at], R. Reed [x], H.G. Ritter [w], J.B. Roberts [ak], O.V. Rogachevskiy [r], J.L. Romero [e],
L. Ruan [c], J. Rusnak [k], O. Rusnakova [j], N.R. Sahoo [as], P.K. Sahu [n], S. Salur [al], J. Sandweiss [bf],
J. Schambach [at], A.M. Schmah [w], W.B. Schmidke [c], N. Schmitz [y], B.R. Schweid [aq], J. Seger [i],
M. Sergeeva [f], R. Seto [ay], P. Seyboth [y], N. Shah [ap], E. Shahaliev [r], P.V. Shanmuganathan [x],
M. Shao [an], W.Q. Shen [ap], F. Shen [ao], Z. Shi [w], S.S. Shi [g], Q.Y. Shou [ap], E.P. Sichtermann [w],
R. Sikora [a], M. Simko [k], S. Singha [s], D. Smirnov [c], N. Smirnov [bf], W. Solyst [o], P. Sorensen [c],
H.M. Spinka [b], B. Srivastava [ai], T.D.S. Stanislaus [bb], D.J. Stewart [bf], M. Strikhanov [aa],
B. Stringfellow [ai], A.A.P. Suaide [am], T. Sugiura [aw], M. Sumbera [k], B. Summa [ag], X.M. Sun [g],
X. Sun [g], Y. Sun [an], B. Surrow [ar], D.N. Svirida [p], A.H. Tang [c], Z. Tang [an], A. Taranenko [aa],
T. Tarnowsky [z], J. Thäder [w], J.H. Thomas [w], A.R. Timmins [au], D. Tlusty [ak], T. Todoroki [c],
M. Tokarev [r], C.A. TomKiel [x], S. Trentalange [f], R.E. Tribble [as], P. Tribedy [c], S.K. Tripathy [n],
B.A. Trzeciak [j], O.D. Tsai [f], B. Tu [g], T. Ullrich [c], D.G. Underwood [b], I. Upsal [ad], G. Van Buren [c],
J. Vanek [k], A.N. Vasiliev [ah], I. Vassiliev [l], F. Videbæk [c], S. Vokal [r], S.A. Voloshin [be], A. Vossen [o],
F. Wang [ai], G. Wang [f], Y. Wang [av], Y. Wang [g], J.C. Webb [c], G. Webb [c], L. Wen [f], G.D. Westfall [z],
H. Wieman [w], S.W. Wissink [o], R. Witt [ba], Y. Wu [s], Z.G. Xiao [av], W. Xie [ai], G. Xie [h], Z. Xu [c],
J. Xu [g], Q.H. Xu [ao], Y.F. Xu [ap], N. Xu [w], C. Yang [ao], S. Yang [c], Q. Yang [ao], Y. Yang [ac], Z. Ye [h],
Z. Ye [h], L. Yi [bf], K. Yip [c], I.-K. Yoo [aj], N. Yu [g], H. Zbroszczyk [bd], W. Zha [an], J.B. Zhang [g],
X.P. Zhang [av], S. Zhang [ap], Z. Zhang [ap], L. Zhang [g], J. Zhang [v], J. Zhang [w], Y. Zhang [an],
S. Zhang [an], J. Zhao [ai], C. Zhong [ap], C. Zhou [ap], L. Zhou [an], Z. Zhu [ao], X. Zhu [av], M. Zyzak [l]

[a] *AGH University of Science and Technology, FPACS, Cracow 30-059, Poland*
[b] *Argonne National Laboratory, Argonne, IL 60439*
[c] *Brookhaven National Laboratory, Upton, NY 11973*
[d] *University of California, Berkeley, CA 94720*
[e] *University of California, Davis, CA 95616*
[f] *University of California, Los Angeles, CA 90095*
[g] *Central China Normal University, Wuhan, Hubei 430079*
[h] *University of Illinois at Chicago, Chicago, IL 60607*
[i] *Creighton University, Omaha, NE 68178*
[j] *Czech Technical University in Prague, FNSPE, Prague, 115 19, Czech Republic*
[k] *Nuclear Physics Institute AS CR, Prague 250 68, Czech Republic*
[l] *Frankfurt Institute for Advanced Studies FIAS, Frankfurt 60438, Germany*
[m] *Fudan University, Shanghai, 200433*
[n] *Institute of Physics, Bhubaneswar 751005, India*
[o] *Indiana University, Bloomington, IN 47408*
[p] *Alikhanov Institute for Theoretical and Experimental Physics, Moscow 117218, Russia*
[q] *University of Jammu, Jammu 180001, India*
[r] *Joint Institute for Nuclear Research, Dubna, 141 980, Russia*
[s] *Kent State University, Kent, OH 44242*
[t] *University of Kentucky, Lexington, KY 40506-0055*
[u] *Lamar University, Physics Department, Beaumont, TX 77710*
[v] *Institute of Modern Physics, Chinese Academy of Sciences, Lanzhou, Gansu 730000*
[w] *Lawrence Berkeley National Laboratory, Berkeley, CA 94720*
[x] *Lehigh University, Bethlehem, PA 18015*
[y] *Max-Planck-Institut fur Physik, Munich 80805, Germany*
[z] *Michigan State University, East Lansing, MI 48824*
[aa] *National Research Nuclear University MEPhI, Moscow 115409, Russia*
[ab] *National Institute of Science Education and Research, HBNI, Jatni 752050, India*
[ac] *National Cheng Kung University, Tainan 70101*
[ad] *Ohio State University, Columbus, OH 43210*
[ae] *Institute of Nuclear Physics PAN, Cracow 31-342, Poland*
[af] *Panjab University, Chandigarh 160014, India*
[ag] *Pennsylvania State University, University Park, PA 16802*
[ah] *Institute of High Energy Physics, Protvino 142281, Russia*
[ai] *Purdue University, West Lafayette, IN 47907*
[aj] *Pusan National University, Pusan 46241, Republic of Korea*
[ak] *Rice University, Houston, TX 77251*
[al] *Rutgers University, Piscataway, NJ 08854*
[am] *Universidade de Sao Paulo, Sao Paulo, 05314-970, Brazil*
[an] *University of Science and Technology of China, Hefei, Anhui 230026*
[ao] *Shandong University, Jinan, Shandong 250100*
[ap] *Shanghai Institute of Applied Physics, Chinese Academy of Sciences, Shanghai 201800*
[aq] *State University of New York, Stony Brook, NY 11794*
[ar] *Temple University, Philadelphia, PA 19122*
[as] *Texas A&M University, College Station, TX 77843*
[at] *University of Texas, Austin, TX 78712*

au *University of Houston, Houston, TX 77204*
av *Tsinghua University, Beijing 100084*
aw *University of Tsukuba, Tsukuba, Ibaraki 305-8571, Japan*
ax *Southern Connecticut State University, New Haven, CT 06515*
ay *University of California, Riverside, CA 92521*
az *University of Heidelberg, Heidelberg, 69120, Germany*
ba *United States Naval Academy, Annapolis, MD 21402*
bb *Valparaiso University, Valparaiso, IN 46383*
bc *Variable Energy Cyclotron Centre, Kolkata 700064, India*
bd *Warsaw University of Technology, Warsaw 00-661, Poland*
be *Wayne State University, Detroit, MI 48201*
bf *Yale University, New Haven, CT 06520*

A R T I C L E   I N F O

A B S T R A C T

Flow harmonics (v_n) in the Fourier expansion of the azimuthal distribution of particles are widely used to quantify the anisotropy in particle emission in high-energy heavy-ion collisions. The symmetric cumulants, $SC(m, n)$, are used to measure the correlations between different orders of flow harmonics. These correlations are used to constrain the initial conditions and the transport properties of the medium in theoretical models. In this Letter, we present the first measurements of the four-particle symmetric cumulants in Au+Au collisions at $\sqrt{s_{NN}} = 39$ and 200 GeV from data collected by the STAR experiment at RHIC. We observe that v_2 and v_3 are anti-correlated in all centrality intervals with similar correlation strengths from 39 GeV Au+Au to 2.76 TeV Pb+Pb (measured by the ALICE experiment). The v_2–v_4 correlation seems to be stronger at 39 GeV than at higher collision energies. The initial-stage anti-correlations between second and third order eccentricities are sufficient to describe the measured correlations between v_2 and v_3. The best description of v_2–v_4 correlations at $\sqrt{s_{NN}} = 200$ GeV is obtained with inclusion of the system's nonlinear response to initial eccentricities accompanied by the viscous effect with $\eta/s > 0.08$. Theoretical calculations using different initial conditions, equations of state and viscous coefficients need to be further explored to extract η/s of the medium created at RHIC.

1. Introduction

High-energy heavy-ion collisions at the Relativistic Heavy Ion Collider (RHIC) and the Large Hadron Collider (LHC) are believed to have created a QCD medium at extremely high energy densities. The properties of this medium are under persistent investigations. An extensively studied subject is "flow", the collective anisotropic expansion of the medium. Flow originates from the initial spatial anisotropy (and/or fluctuations in the position) of the colliding nucleons, and develops due to the strong interaction among particles produced in the collision [1–6]. The anisotropy in the momentum space is quantified by the Fourier coefficients of the azimuthal emission distribution of produced particles with respect to the nth order event plane [7,8]:

$$\frac{dN}{d\varphi} \propto 1 + \sum_{n=1}^{\infty} 2v_n \cos\left[n(\varphi - \Psi_n)\right], \qquad (1)$$

where φ is the azimuthal particle emission angle and Ψ_n is nth order event plane angle. These v_n are the single-particle Fourier coefficients that can be derived without the determination of the event plane which is discussed later on. The flow harmonics, v_n, quantify the nth order anisotropy of particles of interest, and its magnitude imprints the initial anisotropy [1], the expansion dynamics [9,10] and the equation of state of the medium [2,11]. Various efforts have been made to understand the measured flow harmonics and extract the transport properties of the medium, but different models need a different value of η/s (viscosity over entropy density) to describe the same experimental measurements [12,13]. For example, the NeXSPheRIO model with $\eta/s = 0$ (described in Ref. [12]) explains all v_n in all centralities whereas

the MUSIC model (described in Ref. [13]) indicates that a viscous medium with $\eta/s \sim 0.08$ is needed to explain the v_n data in Au+Au collisions at $\sqrt{s_{NN}} = 200$ GeV. This suggests that besides the choice for η/s, other transport properties, equation of state, and the initial state also affects these calculations and using only v_n data it is difficult to have control on these parameters. Therefore, more inputs from experimental observables are warranted to further constrain theoretical models.

To probe the initial conditions, it is important to measure the distributions of v_n and event-by-event correlations among v_n values in an event sample [14,15] as the event-by-event correlations between different orders of flow harmonics are theorized to be sensitive to the transport properties of the medium [16,17]. Recently, the four-particle symmetric cumulants [18–22] have been proposed to unravel the initial-stage phenomena and the later-stage medium properties. These four-particle symmetric cumulants $SC(m, n)$ are defined as [18]

$$
\begin{aligned}
SC(m, n) &\equiv \langle\langle\cos(m\varphi_1 + n\varphi_2 - m\varphi_3 - n\varphi_4)\rangle\rangle_c \\
&= \langle\langle\cos(m\varphi_1 + n\varphi_2 - m\varphi_3 - n\varphi_4)\rangle\rangle \\
&\quad - \langle\langle\cos[m(\varphi_1 - \varphi_2)]\rangle\rangle \langle\langle\cos[n(\varphi_1 - \varphi_2)]\rangle\rangle \\
&= \left\langle v_m^2 v_n^2 \right\rangle - \left\langle v_m^2 \right\rangle \left\langle v_n^2 \right\rangle.
\end{aligned}
\qquad (2)
$$

Here subscript c is used to indicate the cumulant and $\langle\rangle$ denotes average over all events weighted with the number of quadruplet (doublet) combinations. The $\langle\langle\rangle\rangle$ denotes the average over all distinct particle quadruplets (doublets) in an event and over all events weighted with the number of quadruplet (doublet) combinations. Positive (negative) values of $SC(m, n)$ suggest the (anti-)correlation

between v_n^2 and v_m^2; in other words, v_n^2 being larger than $\langle v_n^2 \rangle$ in an event enhances (suppresses) the probability of v_m^2 being larger than $\langle v_m^2 \rangle$ in that same event. The $SC(m,n)$ observables focus on the correlations between different orders of flow harmonics, and facilitate the quantitative comparison between experimental data and model calculations. A normalized symmetric cumulant will facilitate a quantitative comparison between different collision energies or between data and model calculations as the magnitude of symmetric cumulant depends on magnitude of flow harmonics. The normalized symmetric cumulant, $NSC(m,n)$, is defined as

$$NSC(m,n) = \frac{\langle v_n^2 v_m^2 \rangle - \langle v_n^2 \rangle \langle v_m^2 \rangle}{\langle v_n^2 \rangle \langle v_m^2 \rangle}. \tag{3}$$

The ALICE collaboration has recently measured $SC(2,3)$ and $SC(2,4)$ in Pb+Pb collisions at $\sqrt{s_{NN}} = 2.76$ TeV, and found that the centrality dependence of $SC(2,4)$ cannot be captured by hydrodynamics model calculations with a constant η/s [19]. In this Letter, we present the first measurements of symmetric cumulants in Au+Au collisions at $\sqrt{s_{NN}} = 39$ and 200 GeV. Due to limited statistics, results from Au+Au collisions at $\sqrt{s_{NN}} = 62.4$ GeV are not presented in this letter. Section 2 discusses experiment details and the analysis method, and Section 3 describes the results for $SC(2,3)$ and $SC(2,4)$ as functions of centrality and compares them with available model predictions. The summary is in Section 4.

2. Experiment and analysis

The data used in this measurement were collected from Au+Au collisions by the STAR [23] in the years 2010 (39 GeV) and 2011 (200 GeV). We analyzed 1.1×10^8 and 4×10^8 minimum-bias Au+Au events at $\sqrt{s_{NN}} = 39$ and 200 GeV, respectively. The collision centrality determination was validated by comparing Monte Carlo Glauber calculations to the charged-hadron multiplicity measured with the time projection chamber (TPC) within a pseudorapidity window of $|\eta| < 0.5$. The detailed procedures to obtain the simulated multiplicity are similar to that described in Ref. [24]. Events were required to have collision vertex positions (in the radial direction) within 2 cm of the beam axis to reduce contributions from beam-pipe (at a radius of 4 cm) interactions, and within a limited distance from the center of the detector along the beam direction (± 40 cm for the 39 GeV data set and ± 30 cm for the 200 GeV data set). Charged particles used in this analysis were reconstructed by the STAR TPC with $|\eta| < 1.0$. The distance of closest approach (DCA) of a track to the primary vertex was required to be less than 3 cm. We also required the number of fit points (nhits) used to reconstruct a track to be greater than 15 and the ratio of the number of fit points to maximum possible hits (nhits/hitmax) to be greater than 0.52. In addition we applied a transverse momentum cut ($0.2 < p_T < 2$ GeV/c) to the charged tracks to minimize nonflow effects e.g. low and high p_T cuts used to minimize resonance and jet contribution, respectively. These default cut settings were later varied for a systematic analysis.

The two- and four-particle correlations in Eq. (2) can be evaluated in terms of flow vectors [25]. The flow vector (or Q vector) for nth harmonic is defined as $Q_{n,p} \equiv \sum_{k=1}^{M} w_k^p e^{in\varphi_k}$, where M is the multiplicity of an event. The weights ($w_k = w_{\mathrm{eff}} w_\varphi$) were applied to correct for the p_T-dependent efficiency ($w_{\mathrm{eff}} = \frac{1}{\mathrm{eff}(p_T)}$) and for imperfections in the detector acceptance (w_φ). The event-by-event v_n^2 and $v_n^2 v_m^2$ in Eq. (2) were calculated with the multi-particle Q-cumulant method [18,25]:

$$v_n^2 = \langle \cos[n(\varphi_1 - \varphi_2)] \rangle = \frac{\mathrm{N}\langle 2 \rangle_{n,-n}}{\mathrm{D}\langle 2 \rangle_{n,-n}} \tag{4}$$

and

$$
\begin{aligned}
v_n^2 v_m^2 &= \langle \cos(m\varphi_1 + n\varphi_2 - m\varphi_3 - n\varphi_4) \rangle \\
&= \frac{\mathrm{N}\langle 4 \rangle_{n,m,-n,-m}}{\mathrm{D}\langle 4 \rangle_{n,m,-n,-m}},
\end{aligned} \tag{5}
$$

where

$$\mathrm{N}\langle 2 \rangle_{n,-n} = Q_{n,1} Q_{-n,1} - Q_{0,2}, \tag{6}$$

$$\mathrm{D}\langle 2 \rangle_{n_1,n_2} = \mathrm{N}\langle 2 \rangle_{0,0} = Q_{0,1}^2 - Q_{0,2}, \tag{7}$$

$$
\begin{aligned}
\mathrm{N}\langle 4 \rangle_{n,m,-n,-m} =\ & Q_{n,1} Q_{m,1} Q_{-n,1} Q_{-m,1} - Q_{n+m,2} Q_{-n,1} Q_{-m,1} \\
& - Q_{m,1} Q_{0,2} Q_{-m,1} - Q_{n,1} Q_{m-n,2} Q_{-m,1} \\
& + 2 Q_{m,3} Q_{-m,1} - Q_{m,1} Q_{-n,1} Q_{n-m,2} \\
& + Q_{m-n,2} Q_{n-m,2} - Q_{n,1} Q_{-n,1} Q_{0,2} + Q_{0,2} Q_{0,2} \\
& + 2 Q_{-n,1} Q_{n,3} - Q_{n,1} Q_{m,1} Q_{-n-m,2} \\
& + Q_{n+m,2} Q_{-n-m,2} + 2 Q_{m,1} Q_{-m,3} \\
& + 2 Q_{n,1} Q_{-n,3} - 6 Q_{0,4},
\end{aligned} \tag{8}
$$

$$
\begin{aligned}
\mathrm{D}\langle 4 \rangle_{n,m,-n,-m} &= \mathrm{N}\langle 4 \rangle_{0,0,0,0} \\
&= Q_{0,1}^4 - 6 Q_{0,1}^2 Q_{0,2} + 3 Q_{0,2}^2 \\
&\quad + 8 Q_{0,1} Q_{0,3} - 6 Q_{0,4}
\end{aligned} \tag{9}
$$

and

$$Q_{-n,p} = Q_{n,p}^*. \tag{10}$$

The weights of $M(M-1)$ and $M(M-1)(M-2)(M-3)$ were used to average the 2-particle and 4-particle correlations over events (second average in Eq. (2)).

The values of v_n^2 in the denominator of Eq. (3) are obtained with the 2-particle correlations with a pseudorapidity gap of $|\Delta\eta| > 1.0$ between the two particles to suppress few-particle non-flow correlations [20]. The expression of v_n^2 in terms of flow vector with a pseudorapidity gap can be written as

$$v_n^2 = \frac{Q_{n,1}^A \cdot Q_{n,1}^{B*}}{M_A \cdot M_B}. \tag{11}$$

Here $Q_{n,1}^A$ and $Q_{n,1}^B$ are the flow vectors from sub-events A and B, with M_A and M_B the corresponding multiplicities. Although, the eta-gap suppresses few-particle nonflow contributions (mainly due to short range correlation), nonflow due to long range correlations might affect the magnitude of measured normalized $SC(m,n)$.

Reference [26] shows that if $NSC(m,n)$ is measured in a wide centrality range, where the multiplicity significantly fluctuates, the measurements of the symmetric cumulants will be biased by such fluctuations. This is known as the centrality-bin-width (CBW) effect. Accordingly, in this analysis, the symmetric cumulants were measured in small multiplicity windows (bin size equal to one) and then combined into 10% centrality bins to reduce statistical uncertainties. Note that we have checked, using the AMPT model, the magnitude of $NSC(m,n)$ remains unchanged if we use impact parameter bins instead of multiplicity.

The main systematic uncertainties came from 1) event and track selection cuts, and 2) corrections for the non-uniform azimuthal acceptance and efficiency. Two methods were adopted to correct for the azimuthal dependence of the tracking efficiency: φ-weighting and re-centering [7]. In the φ-weighting method, each particle is weighted by the inverse of the corresponding efficiency, w_φ, determined from the particle azimuthal distribution (averaged over many events). In the re-centering method, the event-averaged Q-vector is subtracted from the Q-vector of each event and then the same equations as described above are used. In this analysis,
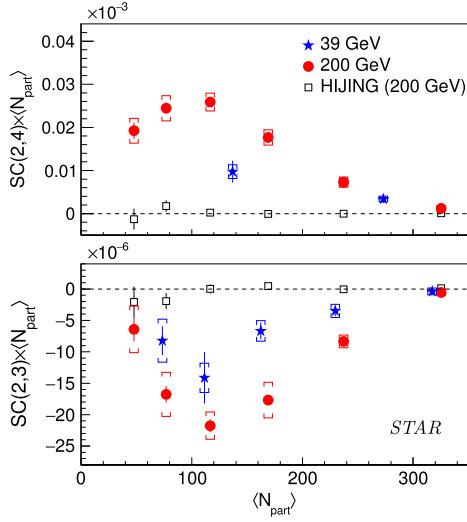
Fig. 1. (Color online.) $SC(2, 4) \times \langle N_{part} \rangle$ and $SC(2, 3) \times \langle N_{part} \rangle$ as functions of $\langle N_{part} \rangle$ in Au+Au collisions at $\sqrt{s_{NN}} = 39$ and 200 GeV. HIJING model results are shown only for 200 GeV. Verticals lines are statistical uncertainties and systematic errors are shown with cap symbols.

Fig. 2. (Color online.) $NSC(2, 4)$ and $NSC(2, 3)$ as functions of $\langle N_{part} \rangle$ in Au+Au collisions at $\sqrt{s_{NN}} = 200$ GeV. The normalized symmetric cumulants of spatial eccentricities, $NSC(m, n)^\varepsilon$, using the Glauber model, are also shown. $NSC(m, n)^v$ represent normalized symmetric cumulants of flow coefficients using equation (3).

the re-centering correction was applied as a function of multiplicity. Both the φ-weighting and the re-centering methods were applied separately for each run period of data taking and centrality interval. The difference between the two correction methods was included in the systematic uncertainty. To estimate systematic uncertainty due to variation of tracks and event selection cuts, we have varied DCA, nhits, nhits/hitmax and Vz values from default cut value. The total systematic uncertainty was obtained by adding uncertainties from different sources in quadrature. Maximum contribution (∼8–12%) to the systematic uncertainty comes from the correction for non-uniform azimuthal acceptance and efficiency.

3. Results

Fig. 1 presents the symmetric cumulants $SC(2, 3)$ and $SC(2, 4)$ multiplied by the average number of participating nucleons, $\langle N_{part} \rangle$, as functions of centrality (represented by $\langle N_{part} \rangle$ [24]) at midrapidity ($|\eta| < 1.0$) for charged hadrons in Au+Au collisions at $\sqrt{s_{NN}} = 39$ and 200 GeV. Systematic errors are shown with cap symbols. Due to limited statistics at 39 GeV, the $SC(2, 4)$ is measured in two wide centrality bins, 0–20% and 20–40%. Positive values of $SC(2, 4)$ are observed for all centrality intervals at both collision energies, suggestive of a correlation between v_2 and v_4. On the other hand, the negative values of $SC(2, 3)$ reveal the anti-correlation between v_2 and v_3. The magnitude of the $SC(2, 3) \times \langle N_{part} \rangle$ and $SC(2, 4) \times \langle N_{part} \rangle$ increases from central to mid-peripheral events and then again decreases for very peripheral events. This is also true for $SC(2, 3)$ and $SC(2, 4)$ (not shown). An inherent feature of the symmetric cumulant is the suppression of nonflow effects thanks to the use of the four-particle cumulant, where nonflow refers to azimuthal correlations not related to the reaction plane orientation, arising from resonances, jets, quantum statistics, and so on. Fig. 1 also shows HIJING model calculations of $SC(2, 3)$ and $SC(2, 4)$ in Au+Au collisions at $\sqrt{s_{NN}} = 200$ GeV [27,28]. Comparison to the HIJING model, which includes only nonflow physics, suggests that nonflow effects cannot explain the data of non-zero symmetric cumulants.

Anisotropic flow is generated by the initial geometric anisotropy coupled with a collective expansion of the produced medium. There is an intense interest in understanding the origin of the initial-stage fluctuations and how these fluctuations manifest
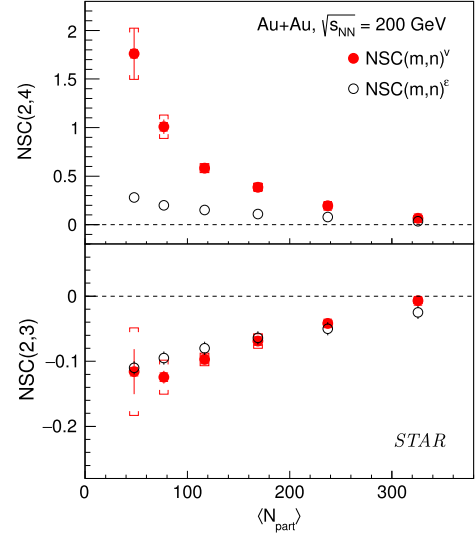
themselves in correlations between measured particles. The normalized symmetric cumulants evaluated in the coordinate space, $NSC(m, n)^\varepsilon = (\langle \varepsilon_n^2 \varepsilon_m^2 \rangle - \langle \varepsilon_n^2 \rangle \langle \varepsilon_m^2 \rangle)/(\langle \varepsilon_n^2 \rangle \langle \varepsilon_m^2 \rangle)$, in Au+Au collisions at $\sqrt{s_{NN}} = 200$ GeV (using the Monte Carlo Glauber model [26]) are shown in Fig. 2 and compared with $NSC(m, n)^v$ measured in the momentum space [7]. If only eccentricity drives v_n, then we expect $NSC(m, n)^v = NSC(m, n)^\varepsilon$. Fig. 2 demonstrates that the initial-stage anti-correlation between the 2nd (ε_2) and 3rd (ε_3) order eccentricity is mainly responsible for the observed anti-correlation between v_2 and v_3. However, the correlation between ε_2 and ε_4 under-predicts the observed correlation between v_2 and v_4. The difference between $NSC(2, 4)^v$ and $NSC(2, 4)^\varepsilon$ increases from central to peripheral collisions. The anisotropic flow v_4 has a contribution not only from the linear response of the system to ε_4, but also has a contribution proportional to ε_2^2. Therefore, the increased difference between $NSC(2, 4)^v$ and $NSC(2, 4)^\varepsilon$ from central to peripheral collisions is presumably because ε_2 has an increased contribution in v_4 in more-peripheral collisions. This is consistent with the observation reported by the ATLAS [29] and ALICE [19] experiments in Pb+Pb collisions at $\sqrt{s_{NN}} = 2.76$ TeV. The relative contribution of ε_2 in v_4, as compared to that of ε_4 was suggested to depend on the viscous properties of the medium [30]. Therefore, $NSC(2, 4)$ provides a probe into the medium properties.

We present the collision energy dependence of the normalized symmetric cumulants $NSC(2, 4)$ and $NSC(2, 3)$ in Fig. 3, as functions of $\langle N_{part} \rangle$. The magnitude of $NSC(2, 4)$ is systematically higher at the lower energy (39 GeV) compared with 200 GeV and 2.76 TeV, though the observed difference is not statistically significant (a ∼2σ effect). This difference could be related to the change in the initial conditions and/or in the transport properties of the medium with collision energy [30,26]. Future high-statistics measurements of $NSC(2, 4)$ at low energies in the phase II of the Beam Energy Scan program (BES-II) at RHIC will further our understanding of the temperature dependence of η/s. The lower panel of Fig. 3 shows a comparison of $NSC(2, 3)$ as a function of centrality between 39 GeV and 200 GeV. The results of $NSC(2, 3)$ at 39 and 200 GeV are consistent with each other. In Fig. 3, the ALICE measurements for 2.76 TeV Pb+Pb [19] are also shown for comparison. Since the ALICE results did not take into account the CBW effect, we have also illustrated the STAR results without the CBW correction (labeled as "Wide Mult. Bins" in Fig. 3) at 200 GeV to make a
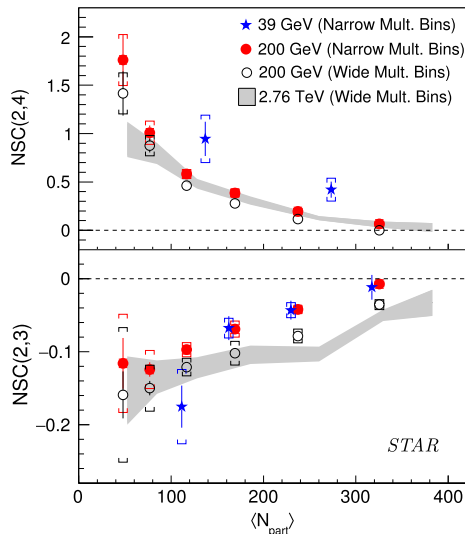
Fig. 3. (Color online.) $NSC(2,4)$ and $NSC(2,3)$ as functions of average $\langle N_{part} \rangle$ in Au+Au collisions at $\sqrt{s_{NN}} = 39$ and 200 GeV. ALICE results for 2.76 TeV Pb+Pb [19] are also shown for comparison. Vertical lines are statistical uncertainties. Systematic errors are shown with cap symbols. The CBW corrected results are labeled by "Narrow Mult. Bins" and CBW uncorrected results are labeled by "Wide Mult. Bins".
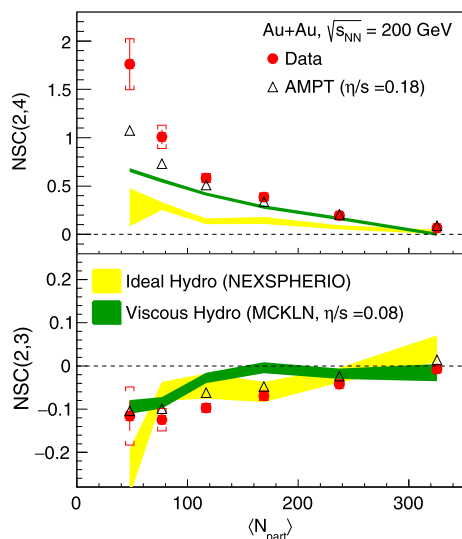

Fig. 4. (Color online.) $NSC(2,4)$ and $NSC(2,3)$ as functions of average $\langle N_{part} \rangle$ in Au+Au collisions at $\sqrt{s_{NN}} = 200$ GeV, with hydrodynamics [26] and AMPT model [21] predictions for comparison. All results are CBW corrected.

fair comparison. There is a slight difference in $NSC(2,4)$ between results with and without the CBW correction; however, this effect is larger in $NSC(2,3)$. The uncorrected values of $NSC(2,3)$ or $NSC(2,4)$ at 200 GeV and 2.76 TeV are very close to each other for all centrality intervals.

We compare in Fig. 4 our measurements with available model predictions [21,26] for $NSC(2,3)$ and $NSC(2,4)$ in Au+Au collisions at 200 GeV. The AMPT calculations [21] are shown for a partonic medium with $\eta/s = 0.18$ (i.e., 3 mb parton–parton interaction cross-section). In the AMPT model, η/s in partonic matter is estimated with the assumption that the partonic matter only consists of massless u and d quarks [31]. AMPT model calculations with $\eta/s = 0.18$ are in agreement with the v_n magnitudes in peripheral collisions, but it over-predicts the v_n data for the most-central collisions [21]. The $NSC(2,3)$ and $NSC(2,4)$ from data are reasonably well described by the AMPT model, however

an increasing deviation between data and AMPT model calculation is observed for $NSC(2,4)$ at peripheral collisions. Predictions from an ideal hydrodynamics model (NexSPheRIO) [26] are also shown in Fig. 4. The ideal hydrodynamics model with NexSPheRIO initial conditions is able to explain the anti-correlation between v_2 and v_3 within theoretical uncertainties, but under-predicts the correlation between v_2 and v_4. The NexSPheRIO model describes the magnitudes of all flow harmonics (v_2, v_3 and v_4) up to $p_T \sim 2.0$ GeV/c within 10%, measured in all centrality intervals at the top RHIC energy [26]. The failure of the ideal hydrodynamics model for the v_2–v_4 correlation supports the idea that the symmetric cumulants provide additional constraints to theoretical models. Like the ideal hydrodynamics model, a viscous hydrodynamics model (MCKLN initial condition and with $\eta/s = 0.08$) roughly explains the $NSC(2,3)$ data and under-predicts $NSC(2,4)$ for peripheral collisions. However, the prediction from the viscous hydrodynamics model for $NSC(2,4)$ is closer to data than the ideal hydrodynamics model. Note that, all presented models (hydro and transport) under-predict $NSC(2,4)$. This may be improved by revisiting model ingredients such as the average initial state, initial state fluctuations, energy deposition "smearing", equation of state, the appearance of other forms of transport, etc. Hence, a sound conclusion requires further investigation along that line.

4. Conclusions

We have presented the first measurements of the charge-inclusive four-particle symmetric cumulants as functions of centrality at midrapidity in Au+Au collisions at $\sqrt{s_{NN}} = 39$ and 200 GeV. The new data provide additional constraints on the initial conditions and the transport properties in theoretical models. Anti-correlation has been observed between event-by-event fluctuations of v_2 and v_3, while the event-by-event fluctuations of v_2 and v_4 are found to be correlated. The initial-stage anti-correlation between ε_2 and ε_3 appears to describe the observed anti-correlation between v_2 and v_3, which seems to support the idea of the linearity between ε_n and v_n [7]. However, the initial-stage correlation alone is not sufficient to describe the measured correlation between v_2 and v_4: the nonlinear hydrodynamic response of the medium has to be included to reproduce the data. The v_2–v_4 correlation seems to be different between 200 GeV and 39 GeV, which could be attributed to the corresponding difference in the initial conditions and/or the transport properties of the medium. We have compared the STAR measurements with a number of available theoretical model calculations. All the models explain the symmetric cumulant between v_2 and v_3; however, none of them are able to describe the v_2–v_4 correlation for all centralities (though the hydrodynamics model ($\eta/s = 0$) could successfully reproduce the individual flow harmonics). A viscous hydrodynamics model with $\eta/s = 0.08$ outperforms the ideal hydrodynamics model in explaining the data, but still seems to under-predict $NSC(2,4)$, whereas the AMPT calculations with $\eta/s = 0.18$ are even closer to the measurement. A detailed comparison of the presented data to models with different equation of states, initial conditions, and transport coefficients is needed to determine these coefficients quantitatively.

References

[1] J.-Y. Ollitrault, Phys. Rev. D 46 (1992) 229.
[2] D. Teaney, J. Lauret, E.V. Shuryak, Phys. Rev. Lett. 86 (2001) 4783.
[3] R.S. Bhalerao, J.-P. Blaizot, N. Borghini, et al., Phys. Lett. B 627 (2005) 49.
[4] R.S. Bhalerao, J.-Y. Ollitrault, Phys. Lett. B 641 (2006) 260.
[5] C. Adler, et al., STAR Collaboration, Phys. Rev. Lett. 87 (2001) 182301.
[6] R. Snellings, New J. Phys. 13 (2011) 055008.
[7] B. Alver, G. Roland, Phys. Rev. C 81 (2010) 054905, Erratum: Phys. Rev. C 82 (2010) 039903.
[8] A.M. Poskanzer, S.A. Voloshin, Phys. Rev. C 58 (1998) 1671.
[9] H. Sorge, Phys. Rev. Lett. 78 (1997) 2309.
[10] P.F. Kolb, P. Huovinen, U. Heinz, et al., Phys. Lett. B 500 (2001) 232.
[11] U. Heinz, J. Phys. Conf. Ser. 50 (2006) 230.
[12] F.G. Gardim, F. Grassi, M. Luzum, et al., Phys. Rev. Lett. 109 (2012) 202302.
[13] B. Schenke, S. Jeon, C. Gale, Phys. Rev. C 85 (2012) 024901.
[14] M. Miller, R. Snellings, arXiv:nucl-ex/0312008.
[15] B. Alver, et al., PHOBOS Collaboration, Phys. Rev. Lett. 98 (2007) 242302.
[16] G. Aad, et al., ATLAS Collaboration, Phys. Rev. C 90 (2014) 024905.
[17] X. Zhu, Y. Zhou, H. Xu, et al., Phys. Rev. C 95 (2017) 044902.
[18] A. Bilandzic, C.H. Christensen, K. Gulbrandsen, et al., Phys. Rev. C 89 (2014) 064904.
[19] J. Adam, et al., ALICE Collaboration, Phys. Rev. Lett. 117 (2016) 182301.
[20] Y. Zhou, K. Xiao, Z. Feng, et al., Phys. Rev. C 93 (2016) 034909.
[21] M. Nasim, Phys. Rev. C 95 (2017) 034905.
[22] A.M. Sirunyan, et al., CMS Collaboration, Phys. Rev. Lett. 120 (2018) 092301.
[23] K.H. Ackermann, et al., STAR Collaboration, Nucl. Instrum. Methods A 499 (2003) 624.
[24] B.I. Abelev, et al., STAR Collaboration, Phys. Rev. C 81 (2010) 024911.
[25] A. Bilandzic, R. Snellings, S. Voloshin, Phys. Rev. C 83 (2011) 044913.
[26] F.G. Gardim, F. Grassi, M. Luzum, et al., Phys. Rev. C 95 (2017) 034901, and private communication.
[27] M. Gyulassy, X.N. Wang, Comput. Phys. Commun. 83 (1994) 307.
[28] X.N. Wang, M. Gyulassy, Phys. Rev. D 44 (1991) 3501.
[29] G. Aad, et al., ATLAS Collaboration, Phys. Rev. C 92 (2015) 034903.
[30] D. Teaney, L. Yan, Phys. Rev. C 86 (2012) 044908.
[31] J. Xu, C.M. Ko, Phys. Rev. C 83 (2011) 034904.